Recurrent Reverse Evolution Maintains Polymorphism after Strong Bottlenecks in Commensal Gut Bacteria

Ana Sousa,[1,2] Ricardo S. Ramiro,[1] João Barroso-Batista,[1] Daniela Güleresi,[1] Marta Lourenço,[‡,1] and Isabel Gordo*[,1]

[1]Instituto Gulbenkian de Ciência, Oeiras, Portugal

[2]Department of Medical Sciences, Institute for Biomedicine, University of Aveiro, Aveiro, Portugal

[‡]Present address: Department of Microbiology, Institute Pasteur, 25-28 Rue du Dr Roux, 75015 Paris, France

***Corresponding author:** E-mail: igordo@igc.gulbenkian.pt.

Associate editor: Deepa Agashe

Abstract

The evolution of new strains within the gut ecosystem is poorly understood. We used a natural but controlled system to follow the emergence of intraspecies diversity of commensal *Escherichia coli*, during three rounds of adaptation to the mouse gut (~1,300 generations). We previously showed that, in the first round, a strongly beneficial phenotype (loss-of-function for galactitol consumption; *gat*-negative) spread to >90% frequency in all colonized mice. Here, we show that this loss-of-function is repeatedly reversed when a *gat*-negative clone colonizes new mice. The regain of function occurs via compensatory mutation and reversion, the latter leaving no trace of past adaptation. We further show that loss-of-function adaptive mutants reevolve, after colonization with an evolved *gat*-positive clone. Thus, even under strong bottlenecks a regime of strong-mutation-strong-selection dominates adaptation. Coupling experiments and modeling, we establish that reverse evolution recurrently generates two coexisting phenotypes within the microbiota that can or not consume galactitol (*gat*-positive and *gat*-negative, respectively). Although the abundance of the dominant strain, the *gat*-negative, depends on the microbiota composition, *gat*-positive abundance is independent of the microbiota composition and can be precisely manipulated by supplementing the diet with galactitol. These results show that a specific diet is able to change the abundance of specific strains. Importantly, we find polymorphism for these phenotypes in indigenous Enterobacteria of mice and man. Our results demonstrate that natural selection can greatly overwhelm genetic drift at structuring the strain diversity of gut commensals and that competition for limiting resources may be a key mechanism for maintaining polymorphism in the gut.

Key words: **experimental evolution, microbiota, reverse evolution, intrastrain polymorphism, nutritional optimization, precision medicine.**

Article

Introduction

The mammalian gut is inhabited by a highly diverse microbial community (including multiple phyla of bacteria, archaea, eukaryotes, and viruses). Current data suggests that maintaining a species rich gut bacterial community is important for multiple aspects of host health (Clemente et al. 2012), including: resistance to pathogens (van Nood et al. 2013), development of the immune system (Faith et al. 2014) and even behavior (Dinan and Cryan 2017). Maintenance of species diversity in the gut may be influenced by several ecological factors: spatial structure (transversal and longitudinal), temporal fluctuations in the environment (e.g., food intake, David et al. 2014) and competitive interactions amongst colonizing species (Coyte et al. 2015). Much less studied is the diversity within each species of the microbiota (Caugant et al. 1981) and the extent to which such intraspecies variation has functional consequences for both bacteria and their hosts (Schloissnig et al. 2013; Greenblum et al. 2015). In particular, the dynamics of emergence and spread of adaptive mutations in commensal gut bacteria are poorly known (Waldor et al. 2015).

Different evolutionary mechanisms can promote genetic diversity within species (Chesson 2000). The recurrent emergence of new adaptive mutations in different clones that compete for fixation—clonal interference—leads to unstable levels of polymorphism (Gerrish and Lenski 1998). On the other hand, resource partitioning and negative-frequency dependent selection leads to stable polymorphisms (Chesson 2000). Evolution by de novo mutation in the gut has recently started to be studied using a mouse model of colonization, the streptomycin-treated mouse. In this model, the antibiotic (streptomycin) is used to deplete some of the microbiota members (the facultative anaerobes) so that specific strains of commensal or pathogenic bacteria can colonize the gut (Krogfelt et al. 2004). Clonal interference (Barroso-Batista et al. 2014; Lourenço et al. 2016), trade-offs between stress resistance and nutritional competence (De Paepe et al. 2011) and negative frequency-dependent selection

(Lourenço et al. 2016), have all been shown to affect the adaptive dynamics of newly emerging mutations in the guts of mice.

The long-term success of bacterial lineages also depends on their ability to transmit between hosts. Such transmission can be vertical, for example, from mother to offspring, or horizontal, for example, in the case of fecal transplantation or migration of microbes between hosts inhabiting the same environment. The process of transmission can entail strong population bottlenecks that may reduce genetic diversity, potentially breaking interactions between strains and/or species that were created within the gut of a given host (Coyte et al. 2015). Genetic diversity can then be regained during population reestablishment. However, it is currently poorly understood whether the recovery in diversity involves mutations that reestablish previously existing polymorphisms at the same or at different loci/traits.

Escherichia coli generally associates with humans as a commensal, being one of the first colonizers of our guts. In particular, the strain K12 constitutes one of the best-studied model organisms. Recently, we began to uncover the nature of the adaptive process that *E. coli* experiences in the gut, by following the evolutionary dynamics of a lineage colonizing mice. Using the streptomycin-treated mouse model of colonization, described above, and a fluorescently labeled strain of *E. coli*, we unraveled the spread of adaptive mutations, by the signature it leaves in the dynamics of neutral fluorescent markers (Barroso-Batista et al. 2014). In this mouse model, the *E. coli* that naturally inhabits the mouse gut, is killed by the antibiotic whereas the fluorescently labeled *E. coli* (which is streptomycin resistant) is able to stably colonize and evolve in the gut. We found that the first step of adaptation to the gut, arising as rapidly as 3 days postcolonization, consisted in the selective inactivation of the operon that allows *E. coli* to metabolize galactitol (i.e., *gat*-negative mutant; Barroso-Batista et al. 2014), a sugar alcohol derived from galactose. Distinct, but phenotypically equivalent, knock-out alleles of this operon bearing a similar selective effect (7.5% benefit; Barroso-Batista et al. 2015) were recurrently observed to emerge across all populations adapting to the gut of independent mice, reaching 95–99% frequency after 24 days (~430 generations). Thus, the fitness effects of mutations comprising the first step of adaptation to the gut could be described by a simple distribution, where all mutations have similar effect (Hegreness et al. 2006).

Here, we use an evolved *gat*-negative single mutant to colonize a new set of mice (mimicking a strong transmission bottleneck), and ask if the rate of adaptation slows down in this complex ecosystem. A deceleration in the rate of adaptation is expected under simple fitness landscape models (Couce and Tenaillon 2015) and is typically found in bacterial populations adapting to laboratory environments (Chou et al. 2011; Khan et al. 2011; Kryazhimskiy et al. 2014). If the selective benefit of emerging mutations decreases during adaptive walks, then diversity might be maintained for longer periods of time. We find that the rate of adaptation does not seem to decelerate for at least two consecutive bouts of adaptation. Unexpectedly, whole-genome sequencing of the evolving populations of the second round of adaptation, revealed that evolution took a step back, with the emergence of multiple mutations that reenabled galactitol metabolism (*gat*-positive) by *E. coli*. These phenotypic reversions occurred by compensatory mutation and genetic reversion. Subsequently, upon a third round of adaptation, using an evolved *gat*-positive strain to colonize new mice, we find de novo loss-of-function mutations. The results demonstrate that in this system, irrespectively of the starting genotype and transmission involving the strongest of bottlenecks, natural selection can maintain polymorphism through recurrent reverse evolution. By assaying microbiota composition and in vivo competitions, we then show that the recurrent reverse evolution leads to the coexistence of two phenotypes whose niches appear to be independent, as they can consume different resources. Furthermore, while the total size of the *E. coli* species is dependent on microbiota composition,—with a more diverse microbiota being associated with a smaller load of *E. coli*—its diversification is not. Indeed, the abundance of the strain that can consume the resource galactitol (*gat*-positive) is relatively constant across mice with distinct microbiota compositions and can be increased by galactitol supplementation, in a concentration dependent manner. Conversely, the abundance of the clones that cannot grow on galactitol (*gat*-negative) is influenced by microbiota composition. Finally, we find that natural isolates of *E. coli*, inhabiting the guts of healthy humans show variation for galactitol consumption—a trait that we find to be under strong selection in laboratory mice.

Results and Discussion

Rate of Adaptation to the Mouse Gut during the Second Steps of Adaptation

We colonized 15 mice with a clonal population of *E. coli* exhibiting the first beneficial phenotype—inability to uptake galactitol—conferred by a single base pair insertion in the coding region of the *gatC* gene, which encodes a subunit of the galactitol transporter. The colonizing population was made dimorphic for a neutral fluorescent marker to allow determination of the spread of further adaptive changes (Hegreness et al. 2006). The time series dynamics of the fluorescent marker frequency resulting from the second steps of adaptation are shown in figure 1A. These dynamics can be summarized in two effective evolutionary parameters (Hegreness et al. 2006; Barrick et al. 2010; Barroso-Batista et al. 2014), the mutation rate (U_e) and the fitness effects of adaptive mutations (S_e) that are estimated to be $U_e = 7.1 \times 10^{-7}$, $S_e = 9\%$ (see Materials and Methods). These quantitatively describe the simplest adaptive scenario where new beneficial mutations emerge at a constant rate and have a constant effect (Hegreness et al. 2006). The estimates of the evolutionary parameters for the second steps of adaptation are remarkably similar to those previously estimated for the first step ($U_e = 7 \times 10^{-7}$, $S_e = 7.5\%$; Barroso-Batista et al. 2014). Direct in vivo competitions between samples of evolved clones and their ancestor (a *gat*-negative strain) further corroborate that the fitness benefit of the accumulated mutations is large, ranging from 5% to 14% fitness increase

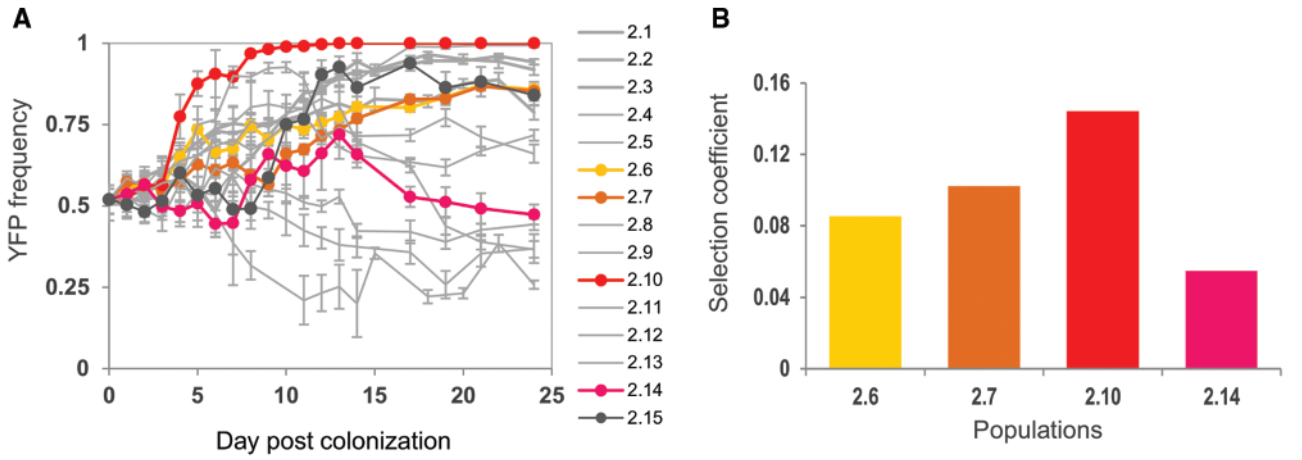

Fig. 1. Rapid adaptation characterizes the evolution of colonizing the mouse gut. (*A*) Change in frequency of a neutral fluorescent marker (YFP) along 24 days of colonization. (*B*) Fitness increase (per generation) measured by direct in vivo competitive assays of evolved clones against the ancestor ($n = 2$).

(mean fitness increase of 9 ± 4% [2SE], fig. 1*B*), which is similar to what was observed for the first steps of adaptation where evolved populations were competed against the ancestral *gat*-positive strain (8 ± 1% [2SE]). Thus, the strength of selection in vivo does not seem to decrease much after the first step of adaptation.

Widespread Reversion of a Strongly Beneficial Mutation upon Transmission

To determine the genetic basis of adaptation underlying the rapid changes in neutral marker frequency (fig. 1*A*), we performed whole genome sequencing (WGS) of samples of two evolving populations along time in two lineages (2.14 and 2.15 from fig. 1*A* and *B*). Remarkably, we uncovered the rapid emergence of several mutations in the galactitol operon (fig. 2*A* and *B*, see also supplementary table S1, Supplementary Material online), particularly in the previously pseudogenized *gatC* (fig. 2*C*). These mutations restored the open reading frame of *gatC* suggesting that an unexpected regain of function could have evolved. Thus, we tested hundreds of evolved clones from these populations for the ability to metabolize galactitol and found that the new mutations in *gatC*, spreading through the populations (fig. 2*A* and *B*), were indeed gain of function mutations. In face of our previous findings (Barroso-Batista et al. 2014), where *gat*-positive *E. coli* evolved a *gat*-negative phenotype that reached >75% frequency in all the mice after 24 days of colonization (fig. 3*A*), the reemergence of the *gat*-positive phenotype was completely unexpected. Indeed, we had assumed that the *gat*-negative phenotype would eventually fix in all populations and therefore started a second colonization with a single adaptive *gat*-negative mutant. This design, mimicking a strong bottleneck or transmission event, serendipitously revealed that evolution could reverse.

To query whether the two populations studied reflect widespread reversion (Porter and Crandall 2003), we tested large samples of clones from all the evolved populations for a *gat*-positive phenotype. We found that phenotypic reversion was highly probable, as in 80% of the 15 independently colonized mice the bacteria regained the ability to consume galactitol, with this phenotype reaching a detectable frequency of at least 0.3% and up to 77% in the evolving populations (fig. 3*B*). Thus, under a transmission event involving a single clone, reacquisition of polymorphism at the *gat* locus constituted a highly predictable adaptive event. Interestingly, the power of selection on this regain of function is clearly observed in population 2.14 (fig. 2*A*), where an allele (involving a 1 bp deletion, the only mutation detected by WGS of the population as indicated in supplementary table S1, Supplementary Material online) emerges in this population at day 11, on the YFP background, but will then compete with a CFP clone which acquired another mutation causing the same phenotype. Thus, the emergence of a *gat*-positive phenotype in both fluorescent backgrounds within the same evolving population (fig. 2*A*) and the parallelism across independent replicate populations (fig. 3*B*) strongly supports the adaptive nature of the regain of function in this ecosystem (de Visser and Krug 2014). To provide further evidence for selection acting on mutations conferring the *gat*-positive phenotype, in contrast to being hitchhiker alleles, we sequenced two *gat*-positive clones. Genome sequencing of the two clones (isolated from population 2.15 at day 6) revealed that: a back-mutation ("rev allele" in fig. 2*C*) had occurred in one clone, with no other mutations detected in its genome; a compensatory mutation ("comp3 allele" in fig. 2*C*), that redoes the open reading frame of *gatC* had occurred in the other clone, whose genome carried no further mutations. These results suggest that the *gat*-positive phenotype is intrinsically beneficial. Moreover, the rare event of gain-of-function through back-mutation could even be observed in one of the assayed populations (2.15, fig. 2*B* and *C*), supporting the conclusion that the ancestral gene can invade a population where loss of function at this locus had previously evolved. Such an event is particularly important since it erases the signature of the strong past selection that had occurred.

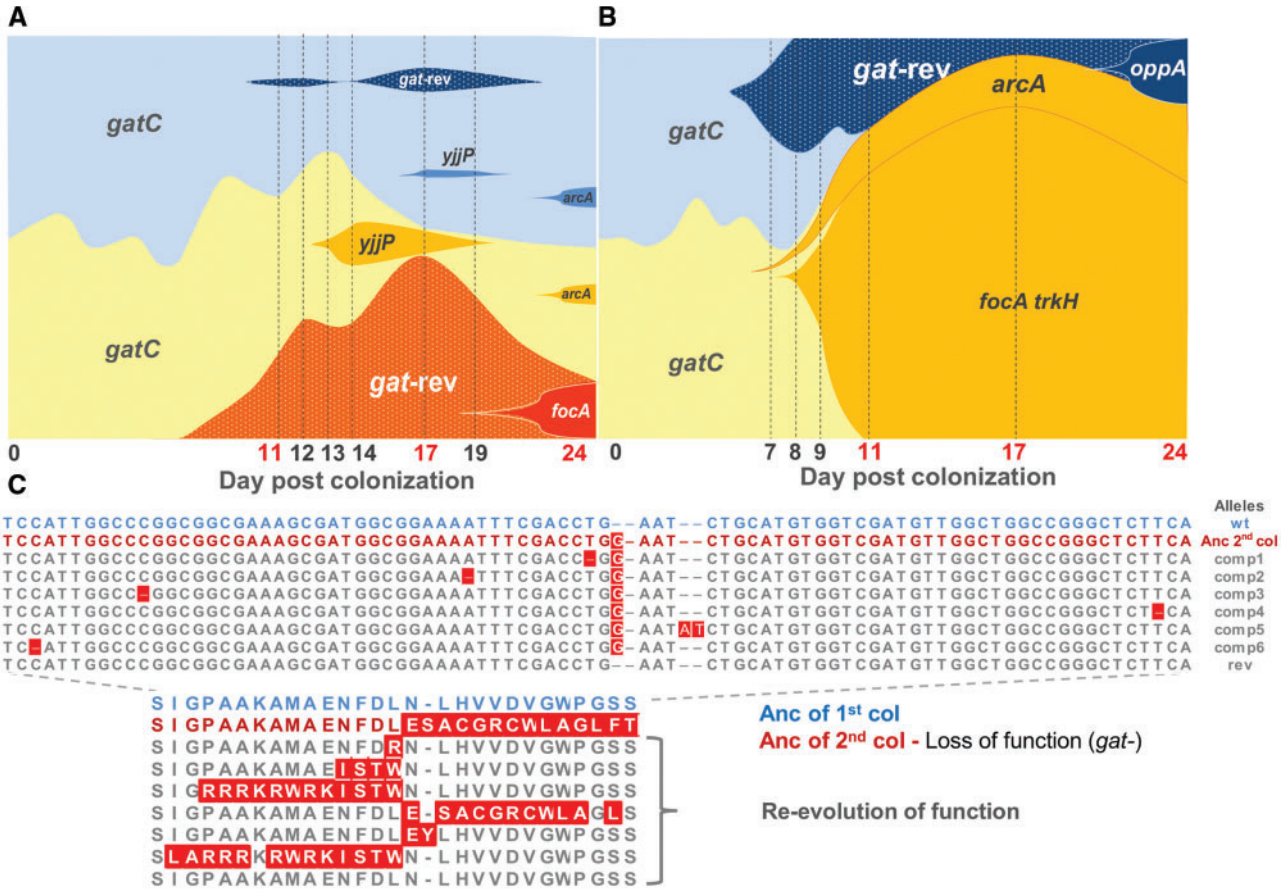

FIG. 2. Reverse evolution leads to the recurrent regain of a previously lost phenotype, by compensatory and back-mutation. (*A* and *B*) Muller Plots showing the emergence of polymorphism in two evolving populations (pop 2.14 (*A*) and pop 2.15 (*B*)), as numbered in fig. 1A) where regain of function (ability to metabolize galactitol) is detected—*gat*-rev. Yellow and blue shaded areas are proportional to the frequencies of YFP- and CFP-labeled bacteria. Darker tones of yellow and blue denote the accumulation of adaptive mutations in the respective background. Days shown below the graph depict the temporal points where haplotype frequencies were estimated (see supplementary table S1, Supplementary Material online) through a combination of different approaches. Numbers in red represent temporal points where frequencies were estimated by WGS of the population and numbers in black represent time points where frequencies were obtained by target PCR of collections of clones. Dotted areas represent the proportion of the population that reverted the ancestral *gat*-negative phenotype and was determined by phenotypic testing. (*C*) The genetic basis of the *gat*-reversion phenotype (*gat*-rev) involves both compensatory (represented by alleles comp1–6) and back-mutation (allele rev). Six different alleles were found in pop 2.14 at day 11 (comp1 to comp6). After 6 days (day17) only alleles comp1 (~1% frequency) and comp2 (~13% frequency) could be detected by WGS; we note however that the frequency of *gat*-rev phenotype in the same time-point was considerably higher (~50%). This suggests that the polymorphism in the *gatC* locus estimated by WGS was considerably underestimated in this time-point. On day 24, comp2 was the only allele detected. Days 6 and 11 of pop 2.15 revealed two different alleles (comp3 and rev). On day 17 and 24 only the rev allele was found.

Natural Selection Maintains Polymorphism during Multiple Rounds of Transmission

To understand the extent to which selection can overwhelm genetic drift (associated with extreme population bottlenecks at host-to-host transmission) in driving the emergence of intraspecies diversity at this locus, we performed a third colonization. This was initiated with an evolved *gat*-positive clone (isolated from population 2.14—fig. 2A), which carries a 2 bp insertion that redoes the *gatC* reading frame and two mutations at other genomic loci (see Materials and Methods for the exact genotype). In all six colonized mice, emergence of the *gat*-negative phenotype, consistent with inactivation of the *gat* operon, was seen (fig. 3C). In this new genetic background, the emergence of polymorphism at detectable frequencies occurred slightly later than in the first colonization: the median time for *gat*-negative phenotype to reach 5% frequency was 7 days (6.25–7.75, Interquartile range), whereas for the first colonization it was 3 days (2–4, Interquartile range, Mann–Whitney–Wilcoxon Test, $W = 1.5$, $P = 0.0006$). The difference in the time of emergence of the polymorphism could be related with the two additional mutations whose phenotype was not characterized.

The three colonizations together (fig. 3A–C) suggest a model of cycling evolution, where a *E. coli* population can loose genetic diversity due to intense drift, caused by strong bottlenecks during transmission events between hosts, but can readily restore polymorphism at this locus due to strong selection in this ecosystem and high mutation rate (fluctuation tests show mutation rates of: 1.0×10^{-5} per generation [95% CI, $\{6.7 \times 10^{-6}, 4.0 \times 10^{-4}\}$] (Lourenço et al. 2016) for

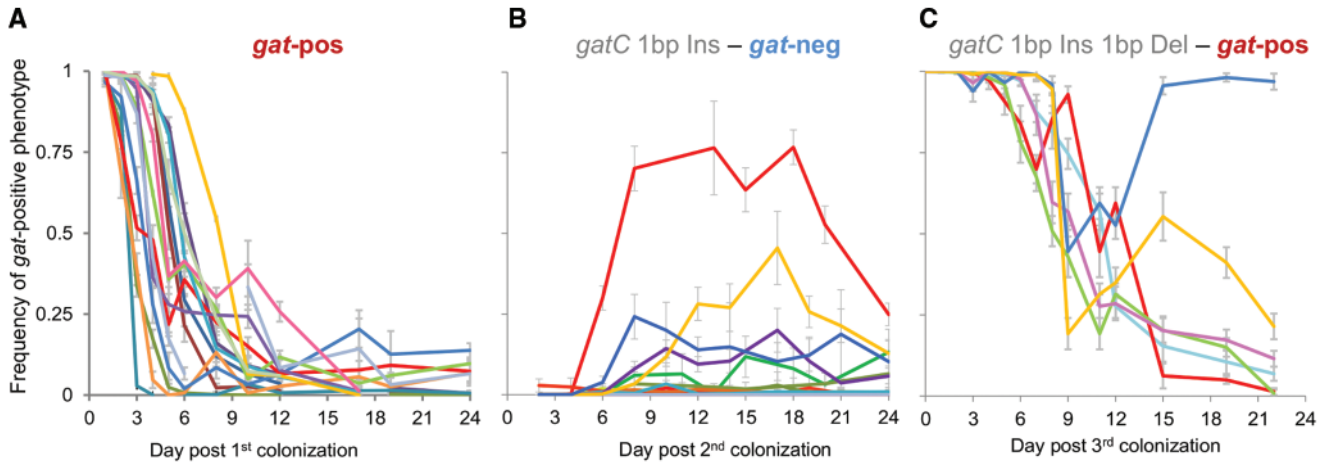

Fig. 3. Reacquisition of the ancestral metabolic ability is pervasive across independently evolving populations. (*A*–*C*) The ancestral genotype and phenotype of each colonization is indicated above the respective graph. (*A*) Massive selection to inactivate the *gat*-operon characterized the first colonization, yet in half of the populations the frequency of *gat*-positive bacteria was kept above 1%. (*B*) In the second colonization, initiated with a *gat*-negative strain, reacquisition of the ancestral metabolic ability was pervasive across independently evolving populations reestablishing the polymorphism for the *gat* phenotype. (*C*) The third colonization, initiated with a *gat*-positive clone isolated from the second colonization, exhibited the reemergence of *gat*-negative mutants, as in the first colonization.

gat-positive to *gat*-negative and 9.7×10^{-9} [95% CI, $\{3 \times 10^{-9}, 1.9 \times 10^{-8}\}$] for *gat*-negative to *gat*-positive [see Materials and Methods]). Such strong bottlenecks may occur during vertical transmission from parent to offspring (Nayfach et al. 2016) and horizontal transmission of pathogenic strains in a hospital setting.

Competition for Limiting Resources Can Help Explaining the Maintenance of Polymorphism at the *gat* Operon

Competition for limiting resources is one of the mechanisms likely to be important in the gut microbial ecosystem (Coyte et al. 2015). Such a mechanism can lead to strong selection for evolving polymorphisms (Chesson 2000). Given the observed polymorphism for galactitol metabolism, we hypothesized that this sugar alcohol could be a key limiting resource for *E. coli* in the mouse gut. Though we did not measure directly the levels of galactitol in the gut, we have explored the potential implications of this being a limiting resource. We first explored the conditions under which a simple resource competition model (Hansen and Hubbell 1980; van Opheusden et al. 2015) could explain the invasions observed in the independent colonizations of figure 3A–C (see Materials and Methods and supplementary fig. S1, Supplementary Material online) and then extended the model to understand the conditions under which a mutant for galactitol metabolism could invade a resident population of bacteria which possesses a regulated operon (see below and supplementary fig. S2, Supplementary Material online). In the simplest model, we assume that the *gat*-negative and the *gat*-positive clones consume two different resources. Given that the *gat*-positive strain (*E. coli* K-12 MG1655) constitutively expresses the *gat* operon (it carries an IS1 insertion in the operon repressor, *gatR*), we further make the simplifying assumption that this strain only consumes one of the resources (galactitol). As expected under these simple assumptions, the theoretical model can reproduce quantitatively the dynamics of emergence of polymorphisms observed in the experiments (supplementary fig. S1*A*, Supplementary Material online). Under these conditions, we expect that supplementation of the mouse diet with galactitol should lead to an increase in frequency of *gat*-positive clones (supplementary fig. S1*B*, Supplementary Material online). To test for this, we colonized new mice with a coculture of *gat*-positive and *gat*-negative bacteria (at a ratio 1:10) while supplementing the mice diet with different concentrations of galactitol. Indeed we observed that the frequency of *gat*-positive bacteria increased in mice drinking water with galactitol ($\chi^2_2 = 31.1$, $P < 0.001$, from day 0 to day 2), and more so when the concentration of galactitol was higher (fig. 4A, also compare with supplementary fig. S1*B*, Supplementary Material online). After day 3, the frequency of *gat*-positive bacteria stabilizes at different levels with different galactitol amounts, with all treatments being significantly different from each other (Tukey tests, $P < 0.0001$). Furthermore, the absolute abundance of the *gat*-positive strain increases with galactitol concentration ($\chi^2_1 = 6.4$, $P = 0.01$; log10 of CFUs: 7.2 ± 0.1, 7.5 ± 0.1 and 8.4 ± 0.03, for 0%, 0.01%, and 0.1% galactitol, respectively, with all treatments being significantly different from each other $P < 0.05$). The total load of *E. coli* was not significantly different across diets ($\chi^2_2 = 4.9$, $P = 0.09$), consistent with the main effect of galactitol supplementation being the increase of *gat*-positive abundance.

We then assayed if the composition of the other species in the mouse gut could be altered when adding galactitol to the diet, by 16S rDNA metagenomics of the mouse fecal samples. Figure 4C shows that the microbiota of the mice drinking galactitol-supplemented water do not cluster separately from those that undergo a normal diet. The same conclusion was reached after performing a PCoA analysis on the data shown in figure 4C, either considering days 3 through 7 (supplementary fig. S6, Supplementary Material online) or each of

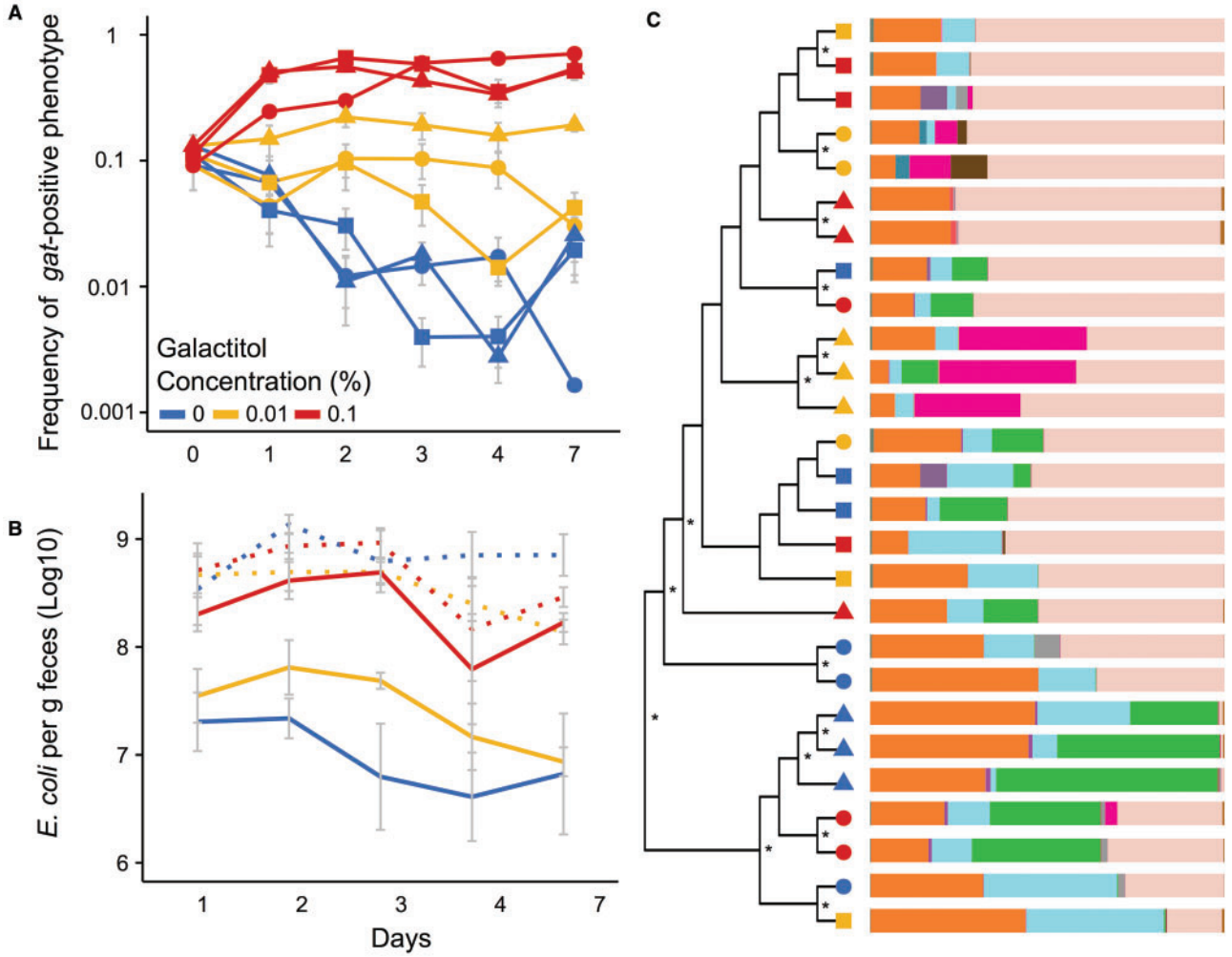

FIG. 4. Diet supplementation with galactitol increases the frequency and abundance of *gat*-positive bacteria, without affecting total *E. coli* density and microbiota composition. Temporal dynamics for the frequency of *gat*-positive *E. coli* (*A*). Temporal dynamics for the density of *gat*-positive (solid lines) and total *E. coli* (dashed lines); error bars correspond to standard error (*B*). Analysis of the mouse gut microbiota shows no evidence for microbiota clustering being influenced by galactitol supplementation (*C*). Dendrogram on the left represents UPGMA clustering of weighted Unifrac (beta diversity), with * indicating when jackknife node support was above 0.9 (100 subsamples of the OTU table). Consistently, alpha diversity is also not influenced by galactitol supplementation (supplementary fig. S5, Supplementary Material online). Bars on the right indicate the relative frequency of the different operational taxonomic units (OTUs; at 97% identity; full legend is provided in supplementary fig. S3, Supplementary Material online). Data from days 3, 4, and 7 was used in this analysis, as after day 3 both the *gat*-positive frequency and the mouse microbiota had started to stabilize (supplementary fig. S4, Supplementary Material online shows the temporal dynamics of gut microbiota per mouse). Colors correspond to: blue—no galactitol supplementation; yellow—0.01% galactitol; red—0.1% galactitol (galactitol was diluted in the mice drinking water). Different symbols correspond to different mice.

the 3 days separately (supplementary fig. S7—day 3, supplementary fig. S8—day 4, and supplementary fig. S9—day 7, Supplementary Material online). Overall, these results suggest that galactitol can increase the frequency of specific strains of *E. coli* (fig. 4*A*) without significantly changing the load of this species (fig. 4*B*) and the relative abundance of other species of the microbiota (fig. 4*C*—within the limits of 16S profiling which is unable to detect differences below the genus level). Nevertheless, we cannot rule out the possibility that galactitol affects the background microbiota in the absence of *E. coli*.

The results so far presented provide a possible explanation for both the emergence and maintenance of polymorphism for galactitol consumption based on the hypothesis of non-overlapping niches. Yet, they do not exclude other hypotheses underlying the recurrent inactivation of the galactitol operon. The *gat*-positive strains which seeded the 1st and 3rd colonization constitutively express the *gat* operon (due to the IS element insertion in the *gatR*) and thus lack regulation. We hypothesized that a strain that could regulate galactitol consumption would be better adapted to the gut, and therefore, mutations that inactivate the *gat* operon would not be selected. To test for this, we replaced the pseudogene *gatR*, in the original strain, by a functional version, which does not impair the ability of consuming galactitol but regulates the operon expression. We then colonized new mice with this strain and followed its evolution in the mouse gut for 19 days ($n = 6$). In contrast to the colonization initiated with *gat*-positive (constitutive), we did not observe the

emergence of *gat*-negative mutants. Therefore, this experiment suggests that the ability to regulate the *gat* operon impedes (or strongly delays) the loss of function previously observed in this ecosystem. Remarkably though, we did observe the emergence of *gat*-constitutive bacteria in all mice colonized with a regulated strain (fig. 5). Furthermore, targeted PCR of the evolved clones showed that the phenotype could be caused by de novo IS insertions in the coding region of *gatR*. Interestingly, these emerging mutants are phenotypically equivalent to the starting *E. coli* clone, which suggests that constitutive mutants might be indeed segregating in natural populations. These results are predicted by the simple model of resource competition (supplementary fig. S2, Supplementary Material online). The observed loss of regulation in vivo is also consistent with previous experiments of adaptation to limiting nutrient concentrations in vitro, in which the repressors of operons for sugar metabolism were inactivated (Horiuchi et al. 1962; Zhong et al. 2004, 2009).

Overall the colonization experiments (figs. 3 and 5) imply that irrespectively of the founder clone being constitutive or regulated, in the long run *gat*-negative and *gat*-positive polymorphism is likely to emerge and be maintained in the gut.

Microbiota Composition Affects *E. coli* Abundance but not *E. coli* Reverse Evolution

The success of *E. coli* colonization, in terms of population size, is variable among mice. On the second colonization, approximately half of the animals are colonized with $\sim 10^8$ CFU/g of feces whereas the other half are colonized with $\sim 10^9$ CFU/g of feces (fig. 6A). This variation could be mediated by the composition of the other members of mouse gut microbiota. We thus enquired whether we could observe an association between the loads of *E. coli* and the microbiota community composition in the gut of the colonized mice (fig. 6A and B). Remarkably, mice with low loads of *E. coli* (fig. 6C) exhibit a microbiota community composition significantly different from mice with high loads of *E. coli* (fig. 6D). Because the great majority of the *E. coli* population is *gat*-negative the same applies to this fraction of the population. In contrast, a remarkable constancy is observed for the abundance of *gat*-positive *E. coli* clones, whose numbers remain around 10^7 CFUs/g irrespectively of microbiota composition. We observed two main microbiota compositions (UPGMA clusters) that we term cluster I and cluster II (I in red and II in blue; fig. 6B–E). Cluster I shows significantly higher species richness (Shannon index $= 4.7 \pm 0.2$ [2SE]; $\chi^2_1 = 13.5$, $P < 0.001$; fig. 6E), being enriched for several OTUs (two Firmicutes and one OTU from Bacteroidetes, Actinobacteria and Deferibacteres; supplementary fig. S10, Supplementary Material online). Cluster II shows a lower Shannon index of 3.3 (± 0.3), being enriched for a single OTU belonging to Actinobacteria (Coriobacteriaceae), Proteobacteria (Entobacteriaceae), and Bacteroidetes (*Bacteroides*). Importantly, cluster I is associated with an abundance of *gat*-negative *E. coli* that decreases overtime, tending to $< 10^8$ (per feces gram), which is significantly lower than that observed in cluster II (with average abundance of 10^9 per feces gram; $\chi^2_1 = 33.6$, $P < 0.001$). These results suggest that

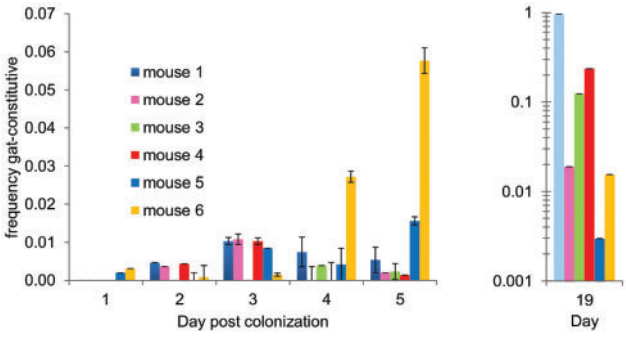

Fig. 5. Emergence of *gat*-constitutive strains in the guts of mice colonized with a clonal population of bacteria where the repressor of the galactitol operon (*gatR*) has been restored. (*A*) Frequency of *gat*-constitutive mutants that emerged de novo in all colonized mice ($n = 6$) during the first 5 days of colonization (*A*). (*B*) Frequency of *gat*-constitutive mutants at day 19 in the same mice.

gat-negative *E. coli* may compete with other members of the microbiota for resources and that the *gat*-positive *E. coli*, which acquired mutations leading to increase expression of the *gat* operon and increased growth on galactitol, may be selected for because they avoid such competition. As galactitol supplementation and the microbiota independently affect the abundances of *gat*-positive and *gat*-negative *E. coli* (respectively), these results appear to suggest that the two phenotypes occupy different niches.

The theoretical model suggests that the equilibrium ratio of *gat*-positive to *gat*-negative is dependent on the relative abundance of galactitol to other undefined resources (see Materials and Methods) and that the abundance of these two phenotypes can vary independently as these consume different resources. Interestingly, in the galactitol supplementation experiment (fig. 4A–C), we see that increasing galactitol concentration leads to an increase in the abundance of *gat*-positive bacteria ($\chi^2_1 = 6.4$, $P = 0.01$), without affecting the abundance of *E. coli* ($P > 0.05$). Conversely, in the colonization experiment (fig. 3B) it is the abundance of *gat*-negative bacteria that varies across mice, whereas the abundance of *gat*-positive bacteria remains relatively constant after their emergence (fig. 6A). This suggests that there is variation in the concentrations of the unidentified resources that are consumed by the *gat*-negative *E. coli*.

Natural Polymorphism for Galactitol Consumption in Indigenous Enterobacteriacea of Mice and Humans

The findings reported here suggest that the gut ecology may favor natural polymorphism for galactitol metabolism in its microbiota. To test for this, we sampled Enterobacteriacea clones from the natural microbiota of our host model organism (fecal samples of mice untreated with antibiotics in the IGC animal house [$n = 20$]) and from the gut microbiota of healthy humans with no controlled diet ($n = 9$). Variation for this trait was found to be segregating across mice and man (table 1). In one out of nine human hosts, polymorphism for the ability to consume galactitol was detected, with 58% of the clones being *gat*-negative. In five humans, the *gat*-negative phenotype was present at frequencies above 90%, with some

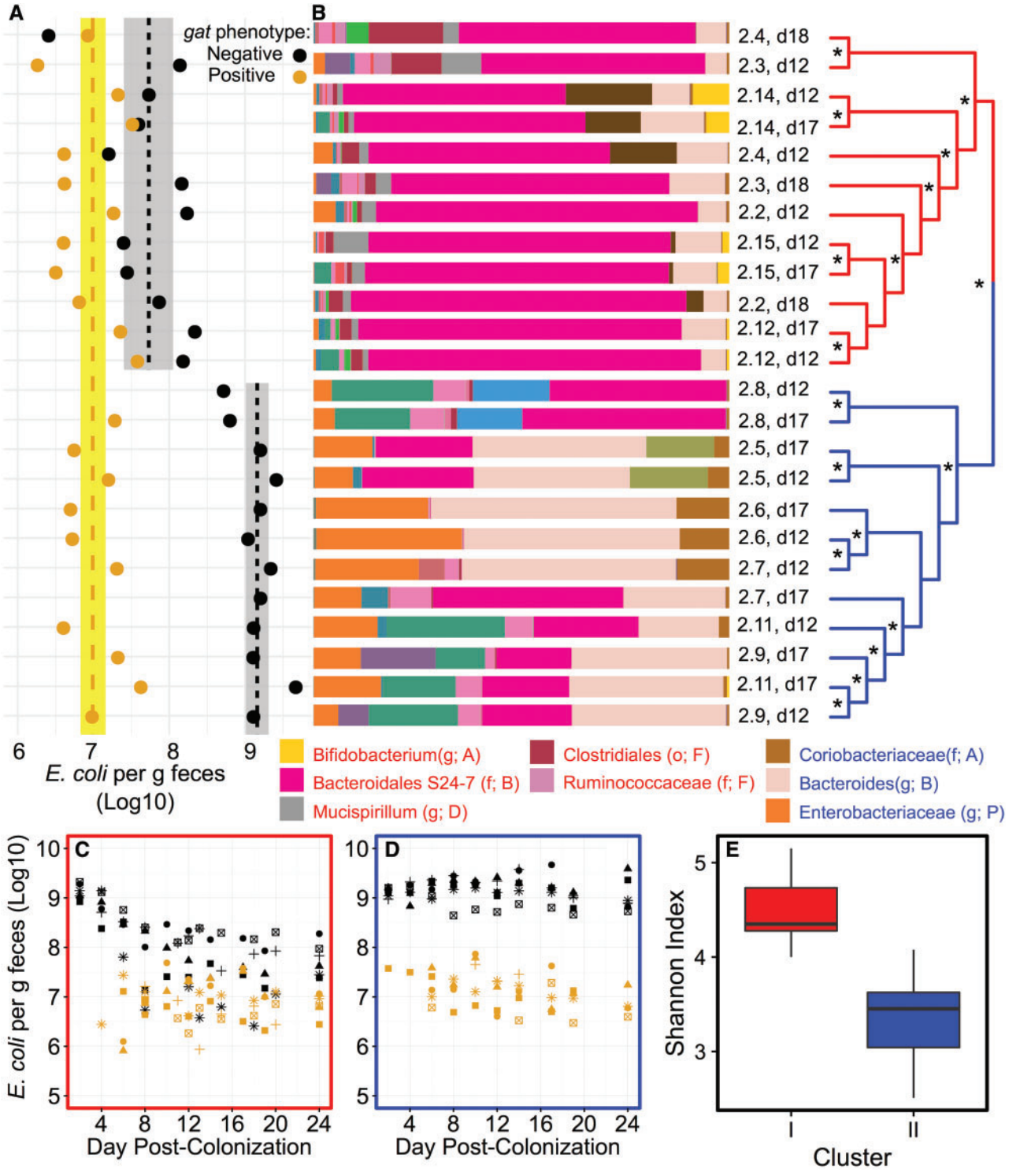

Fig. 6. Microbiota composition affects the density of *gat*-negative, but not *gat*-positive *E. coli*. Microbiome analysis was carried for mice from the second colonization (figs. 1 and 3*B*) in which *gat*-positive revertants had emerged. Moreover, the densities of *gat*-positive and *gat*-negative *E. coli* were estimated. The gut microbiota affects the densities of *gat*-negative but not *gat*-positive *E. coli* (*A*). Dot plots indicate the densities of *E. coli* with each phenotype for the corresponding mouse-day combination. Line and shading indicate the mean and standard error. For *gat*-negative, two lines are shown as the bacterial densities differ significantly between red and blue clusters. Conversely, for *gat*-positive, only one line is shown as there is no significant difference. (*B*) Analysis of the mouse gut microbiota divides mice into two main clusters, I (red) and II (blue). Dendrogram on the right represents UPGMA clustering of weighted Unifrac (beta diversity), with * indicating when jackknife node support was above 0.9 (100 subsamples of the OTU table). Bars on the left indicate the relative frequency of the different operational taxonomic units (OTUs; at 97% identity). Labeled taxa are enriched in either cluster I (red labels) or II (blue labels), as identified by LEfSe (full legend is provided in supplementary fig. S3, Supplementary Material online and LefSe results in supplementary fig. S10, Supplementary Material online). (*C*–*D*) Temporal dynamics of *gat*-negative and *gat*-positive *E. coli* showing that the densities of *gat*-negative *E. coli* are lower in mice with the cluster I microbiota (*C*), than in mice

Table 1. Polymorphism for Galactitol Metabolism in Natural Fecal Isolates.

Sample #		*gat*-pos	*gat*-neg	Total	Frequency of *gat*-neg	2SE
Mouse	1	1	143	144	0.99	0.01
Mouse	2	125	19	144	0.13	0.06
Mouse	3–20	144	0	144	0.00	0.01
Human	1	189	3	192	0.02	0.02
Human	2	12	180	192	0.94	0.03
Human	3	192	0	192	0.00	0.01
Human	4	2	190	192	0.99	0.01
Human	5	11	181	192	0.94	0.03
Human	6	81	111	192	0.58	0.07
Human	7	1	191	192	0.99	0.01
Human	8	19	173	192	0.90	0.04
Human	9	192	0	192	0.00	0.01

showing a frequency of ~99%. Only three humans showed no *gat*-negative Enterobacteriacea. From 20 mice assayed, one was monomorphic for the *gat*-negative phenotype, one showed an intermediate frequency for this phenotype and the rest showed only *gat*-positive clones. These results indicate that the level of polymorphism at this locus may be influenced by antibiotic treatment or the strain background used for gut colonization. Nevertheless, in more natural conditions trait polymorphisms can also be found. Interestingly, in a comparative genomics survey of genes under positive selection in *E. coli*, *gatC* was found to be a target of repeated replacement substitution driven by positive selection (Chattopadhyay et al. 2009).

Conclusions

Overall our results highlight how evolutionary and ecological processes interact to shape the genetic and phenotypic composition of commensal bacteria within a natural ecosystem. At the evolutionary level, we find that a strong-mutation-strong-selection-strong-drift regime of adaptation can lead to the maintenance of polymorphism through frequent episodes of reverse evolution, which defy Dollo's law of evolutionary irreversibility (Gould 1970; Marshall et al. 1994). This regime of adaptation has been poorly studied, at both the theoretical and experimental levels, but may be important for host-associated microbes as their population dynamics often involves transmission bottlenecks (strong-drift) followed by expansion to large population sizes (strong-mutation-strong-selection). Interestingly, reversion has also been shown to rapidly occur for immune escape mutations in HIV (Friedrich et al. 2004). Our study reveals that phenotypic and genetic reversals may be common in bacteria colonizing the mammalian intestine. Such scenario may have been difficult to predict, as bacteria could be expected to respond to changing environments by gene regulation and not through de novo mutation, as we showed here. One context where reversion is pivotal regards antibiotic resistance. Reversion of antibiotic resistant bacteria to sensitivity has been more rarely observed than what one would desire (Andersson and Hughes 2010). However, since most studies have been done in vitro, it would be important to determine if the rate of reversion of resistance in vivo could be as high as the one we found here for a metabolic trait (Björkman et al. 2000).

At the ecological level, our results indicate that resource specialization may allow new emerging strains to avoid competition with other members of the microbiota (Conway and Cohen 2015), even if to stably colonize the gut at low abundances. Our results further highlight that precise dietary supplementations may allow for controlling the colonization level of specific strains.

In sum, the evolutionary invasion and ecological stability of de novo emerging clones in genetic identical hosts, nurtured in identical conditions, was highly reproducible, despite being accompanied by significant differences in the level of microbiota species richness between hosts.

Materials and Methods

Bacterial Strains and Culture Conditions

All strains used in this study were derived from MG1655, a K12 commensal strain of *Escherichia coli* (Blattner et al. 1997).

Ancestors of the First Colonization

The two ancestors of the first colonization (fig. 3A), described in a previous experiment (Barroso-Batista et al. 2014), were DM08-YFP and DM09-CFP (MG1655, *galK::YFP/CFP* amp^R, str^R [*rpsL150*, Δ*lacIZYA*]).

Ancestors of the Second Colonization

Strains JB19-YFP and JB18-CFP (MG1655, *galK::YFP/CFP* cm^R, str^R *(rpsL150)*, Δ*lacIZYA*, Ins (1 bp) *gatC*) were used for the second colonization (fig. 3B) and were previously described in (Lourenço et al. 2016). These strains differ from the ancestral MG1655 fluorescent strains DM08-YFP and DM09-CFP by a mutation in the *gatC* gene (1 bp insertion in the coding region), rendering it unable to metabolize galactitol. To construct these strains, the ampicillin resistance cassette in the ancestral strains DM08-YFP and DM09-CFP was replaced with a chloramphenicol resistant cassette using the Datsenko and Wanner method (Datsenko and Wanner 2000). The yellow (*yfp*) and cyan (*cfp*) fluorescent genes linked to cm^R were then transferred by P1 transduction to a derivative of clone 12YFP (Barroso-Batista et al. 2015), an evolved clone of DM08-YFP, isolated after 24 days of adaptation in the gut of WT mice, that carried an insertion of 1 bp in *gatC* and a large duplication. During the genetic manipulations the large duplication was lost, confirmed by whole genome

Fig. 6. Continued

with the cluster II microbiota (*D*) (cluster: time interaction: $\chi^2_1 = 33.6$, $P < 0.001$). Conversely, the densities of *gat*-positive clones remain constant across all mice (cluster: time interaction: $\chi^2_1 = 3.3$, $P = 0.07$ and cluster single effect: $\chi^2_1 = 1.0$, $P = 0.31$). (*E*) Microbiota diversity (estimated as Shannon Index) is significantly lower in cluster II than in cluster I (similar observations are made for other diversity indices; see supplementary fig. S11, Supplementary Material online).

sequencing, leaving this clone with a single mutation in *gatC* (Lourenço et al. 2016).

Ancestor of the Third Colonization

The strain used to start the third colonization was isolated from population 2.4 of the second colonization at day 24 postcolonization. This strain (named 19CFP (Lourenço et al. 2016) has a 2 bp insertion (+TC) in *gatC* which reconstructed the open reading frame allowing it to recover the ability to consume galactitol (see below details about the phenotype confirmation). Additionally, this strain has the following mutations: an IS2 insertion in the coding region of *ykgB* and a 6,790 bp deletion from gene *intZ* to *eutA*.

Reconstruction of the transcriptional regulator of the galactitol metabolism (*gatR*): the *gatR* coding region is interrupted by an IS element in *E. coli* MG1655, and therefore in all strains used in this study. This insertion inactivates *gatR* leading to the constitutive expression of the *gat*-operon. To restore the function of the gene, and therefore the ability to regulate the operon, a copy of the *gatR* native sequence (obtained from the strain *E. coli* HS) was used to replace the nonfunctional copy. This was accomplished by the *SacB-TetA* counter selection method as previously described (Li et al. 2013). Briefly, the *SacB-TetA* fragment with the overhangs for recombination was obtained by target PCR using the primers *gatR_SacB*_F/*gatR_SacB*_R (supplementary table S2, Supplementary Material online) and genomic DNA of *E. coli* XTL298 as a template. The resulting PCR product was then used to replace the nonfunctional copy of *gatR* present in strains DM08 and DM09 by the Wanner method (Datsenko and Wanner 2000). The DNA fragment containing the native sequence of *gatR* was obtained by target PCR using the primers *yegS*_F/*gatD*_R and *E. coli* HS as a template. Finally, this fragment was used to replace the counter selection cassette in the *gatR* locus of the recipient strains DM08 and DM09 by the Wanner method (Datsenko and Wanner 2000) and plated on double-counter-selective medium. Candidates for successful restoration of *gatR* were screened by PCR and tested for antibiotic resistances to confirm the loss of the cassette and the plasmid before sequencing.

To distinguish between *gat*-negative and *gat*-positive bacteria, we used the differential medium MacConkey agar supplemented with galactitol 1% and streptomycin (100 μg/mL). Plates were incubated at 30 °C. The frequency of *gat*-negative mutants was estimated by counting the number of white (auxotrophic for galactitol) and red colonies. On average around 1,000 colonies per time point were plated to estimate the frequency of *gat*-negative mutants, therefore the minimal frequency detected by this method is ~0.5%.

In Vivo Experimental Evolution

In order to study *E. coli*'s adaptation to the gut we used the classical streptomycin-treated mouse model of colonization (Krogfelt et al. 2013) and performed the evolution experiments using the same conditions as before (Barroso-Batista et al. 2014; Barroso-Batista et al. 2015; Lourenço et al. 2016). Briefly, 6- to 8-week old C57BL/6 male mice raised in specific pathogen free conditions were given autoclaved drinking water containing streptomycin (5 g/L) for 1 day. After 4 h of starvation for water and food, the animals were gavaged with 100 μL of a suspension of 10^8 colony forming units of a mixture of YFP- and CFP-labeled bacteria (ratio 1:1) grown at 37 °C in brain heart infusion medium to OD_{600} of 2. After the gavage, all animals were housed separately and both water with streptomycin and food were returned. Mice fecal samples were collected for 24 days and diluted in PBS, from which a sample was stored in 15% glycerol at −80 °C and the remaining was plated in Luria Broth agar supplemented with streptomycin (LB plates). Plates were incubated overnight at 37 °C after which fluorescent colonies were counted using a fluorescent stereoscope (SteREO Lumar, Carl Ziess) to assess the frequencies of CFP- and YFP-labeled bacteria. These fluorescent proteins are used as neutral markers with which we can follow to detect the emergence of beneficial mutations, since these markers hitchhike with the beneficial mutations that spread in the populations (Hegreness et al. 2006).

In Vivo Competitive Assays

To test the in vivo advantage of the evolving populations at the last time point of the evolution experiment (fig. 1A), samples of either YFP or CFP clones isolated from day 24 (subpopulations) were competed against the respective ancestor labeled with the opposite fluorescent marker ($n = 2$ for each population). These subpopulations were composed of mixtures of ~30 colonies with the same fluorescent marker isolated after plating the appropriate dilution of mice fecal pellets. The mixtures of clones were then grown in 10 mL of LB supplemented with chloramphenicol (100 μg/mL) and streptomycin (100 μg/mL) and stored in 15% glycerol at −80 °C. In vivo competitions of evolved subpopulations against the ancestral were performed at a ratio of 1:1, following the same procedure described above for the evolution experiment. Mice fecal pellets were collected for 3 days, diluted in PBS and frozen in 15% glycerol at −80 °C. Frequencies of CFP- and YFP-labeled bacteria were estimated using a fluorescent stereoscope (SteREO Lumar, Carl Ziess). The selective coefficient (fitness gain) of these mixtures of clones in vivo (presented in fig. 1B) was estimated as: $s_b = ln\left(\frac{Rf_{ev/anc}}{Ri_{ev/anc}}\right)/t$, where s_b is the selective advantage of the evolved clone, $Rf_{ev/anc}$ and $Ri_{ev/anc}$ are the ratios of evolved to ancestral bacteria in the end (f) or in the beginning (i) of the competition and t is the number of generation per day. We assumed $t = 18$ generations, in accordance with the 80 min generation time estimated in previous studies on *E. coli* colonization of streptomycin-treated mouse (Poulsen et al. 1995; Rang et al. 1999).

Whole Genome Resequencing and Mutation Prediction

Clone Analysis

Two *gat*-positive clones (revertant) isolated from the second colonization (day 6 of population 2.15) were sequenced to test for the presence of additional mutations, besides the one reverting the *gat*-phenotype. Two independent colonies were used to inoculate 10 mL of LB and incubated at 37 °C with

agitation for DNA extraction (following a previously described protocol; Wilson 2001). The DNA library construction and sequencing was carried out at the IGC sequencing facility. Each sample was paired-end sequenced on an Illumina Mi Seq Benchtop Sequencer. Standard procedures produced data sets of Illumina paired-end 250 bp read pairs. Genome sequencing data have been deposited in the NCBI Read Archive, https://www.ncbi.nlm.nih.gov/bioproject/PRJNA295680 (last accessed August 18, 2017). Mutations were identified using the BRESEQ pipeline (Deatherage and Barrick 2014). To detect potential duplication events, we used ssaha2 (Ning et al. 2001) with the paired end information. This is a stringent analysis that maps reads only to their unique match (with <3 mismatches) on the reference genome. Sequence coverage along the genome was assessed with a 250 bp window and corrected for GC% composition by normalizing by the mean coverage of regions with the same GC%. We then looked for regions with high differences (>1.4) in coverage. Large deletions were identified based on the absence of coverage. For additional verification of mutations predicted by BRESEQ, we also used the software IGV (version 2.1) (Robinson et al. 2011).

Population Analysis

DNA isolation, library construction, and sequencing were carried as described above for the clone analysis except that now it derived from a mixture of >1,000 clones per population grown in LB agar. Two populations, from the evolution experiment, were sequenced: 2.14 and 2.15. Those were sequenced for three time points during the adaptive period (generation 198 [day 11], generation 306 [day 17], and generation 432 [day 24]). Mean coverage per sample was between ~100× and ~300× for population 2.14 and between ~70× and ~115× for population 2.15. Mutations were identified using the BRESEQ pipeline (version 0.26) with the polymorphism option on. The default settings were used except for: 1) requirement of a minimum coverage of three reads on each strand per polymorphism; 2) eliminating polymorphism predictions occurring in homopolymers of length >3; 3) polymorphism predictions with significant ($P = 0.05$) strand or base quality score bias were discarded. Data presented in supplementary table S1, Supplementary Material online.

Diet Supplementation Experiment

To test the selective pressure exerted by galactitol, when present in the gut, we performed in vivo competitions between *gat*-positive (DM08) and *gat*-negative (JB18) bacteria, whereas supplementing the diet with this sugar. Competition experiments were performed as described above except that the initial frequency of *gat*-positive bacteria was ~10% and the drinking water was supplemented with 0%, 0.01%, or 0.1% of galactitol ($n = 3$ for each galactitol concentration) together with streptomycin (5 g/L). Fecal samples were collected daily and plated to access the frequencies of both phenotypes during 4 days.

Estimate of Gain-of-Function Mutation Rate from *gat*-Negative to *gat*-Positive Phenotype

Strains JB19 (*gatC* 1 bp Ins) and 4YFP (*gatZ* IS Ins) were grown overnight in 10 mL of LB at 37 °C with aeration. After growth, the total number of cells in the cultures was measured by flow cytometry (using BD LSR Fortessa; BD Biosciences) and ~1,000 cells were used to inoculate 1 mL of LB (10 replicates of each strain) and incubated overnight. Aliquots of each replicate tube were plated in LB agar and MM agar supplemented galactitol 1% and incubated overnight at 37 °C. The number of spontaneous *gat*-positive mutants and total number of cells grown on LB were used to estimate the mutation rate using the maximum likelihood approach as implemented in FALCOR (Hall et al. 2009).

We measured the mutation rate to reacquire the ability to consume galactitol, since this locus was previously demonstrated to be a hotspot for loss of function mutations (Lourenço et al. 2016). The fluctuation test revealed that the spontaneous rate at which the ancestor of the second colonization (*gat*-negative) recovers the ability to consume galactitol is 9.7×10^{-9} (95% CI, [3×10^{-9}, 1.9×10^{-8}]) per generation. Considering that the estimated spontaneous rate of small indels in *E. coli* is ~2×10^{-11} (Lee et al. 2012), and that about one third of such mutations in a region of ~30 aminoacids of *gatC* could restore the open reading frame in the ancestral clone of the second colonization, the expected rate of mutation towards a *gat*-positive phenotype is ~6×10^{-10}. This estimate is between 5 and 15 times lower than that observed in the fluctuation assay, suggesting that a high mutation rate may have also contributed to the frequent reemergence of *gat*-positive bacteria in the evolution experiment.

Identification of Adaptive Mutations and Estimate of Haplotype Frequencies in Selected Populations of the Evolution Experiment

In order to estimate the haplotype frequencies depicted in figure 2*A* and *B*, two complementary strategies were employed. In addition to the WGS of the populations, targeted PCR of the identified parallel mutations was performed. For the targeted PCR, 20–80 clones from different time points were screened (from populations 2.14 and 2.15) using the same primers and PCR conditions as in (Barroso-Batista et al. 2014; Lourenço et al. 2016). Because all target mutations correspond to IS insertions an increase in size of the PCR band is indicative of the presence of an IS. Frequency of *gat*-revertant was estimated by plating in differential media (MacConkey supplemented with 1% galactitol). Frequencies are depicted in supplementary table S1, Supplementary Material online.

Microbiota Analysis

We extracted DNA from mice fecal samples from two experiments: the second colonization (fig. 3*B*) and the galactitol supplementation experiment (fig. 4*A* and *B*). For the second colonization, we extracted DNA from mice where *gat*-positive *E. coli* could be detected (12 out of 15), at days 12 and 17 or 18

postcolonization (i.e., two samples per mouse). For the galactitol supplementation experiment, we extracted DNA at days 1, 2, 3, 4, and 7 postcolonization, for the nine mice involved in this experiment. Moreover, we extracted and sequenced a negative control (extraction without feces).

Fecal DNA was extracted with a QIAamp DNA Stool Mini Kit (Qiagen), according to the manufacturer's instructions and with an additional step of mechanical disruption (Thompson et al. 2015). 16 S rRNA gene amplification and sequencing was carried out at the Gene Expression Unit from Instituto Gulbenkian de Ciência, following the service protocol. For each sample, the V4 region of the 16 S rRNA gene was amplified in triplicate, using the primer pair F515/R806, under the following PCR cycling conditions: 94 °C for 3 min, 35 cycles of 94 °C for 60 s, 50 °C for 60 s, and 72 °C for 105 s, with an extension step of 72 °C for 10 min (Caporaso et al. 2011; Caporaso et al. 2012). Samples were then pair-end sequenced on an Illumina MiSeq Benchtop Sequencer, following Illumina recommendations.

QIIME (Caporaso et al. 2010) was used to analyze the 16S rRNA sequences by first quality filtering the samples with a phred quality threshold of 20 (with script split_libraries_fastq) and then OTU picking by assigning operational taxonomic units at 97% similarity against the Greengenes database (DeSantis et al. 2006); using script pick_open_reference_otus with default settings, but enabling reverse strand matches). The OTU table generated by the latter script was then filtered in two steps. First, with script remove_low_confidence_OTUs, from the Microbiome helper repository (Comeau et al. 2017), to remove potentially spurious OTUs. Second, to remove contaminants (Salter et al. 2014) identified in the negative control, we filtered out any OTUs that were present in both the negative control and two or less samples at a frequency <0.01. The OTUs that were kept in the final OTU table and that were shared between negative control and samples had a maximum frequency of 0.004 in the negative control, were present at a frequency of >0.01 in at least five samples and had an average frequency in samples that was at least one order of magnitude higher than the observed in the negative control. The OTU table obtained after these two steps was then used for the analysis below. To understand the clustering pattern of the mouse gut microbiota in each experiment, we used the script jackknifed_beta_diversity to build rarefied OTU tables (at 75% of the minimum read depth in each experiment, as advised on QIIME's website). This built 100 rarefied OTU tables, computed weighted UniFrac (Lozupone and Knight 2005) and generated a consensus tree (per experiment) with jackknife support of tree nodes. Consensus trees were then plotted with R package ggtree together with the OTU relative abundance (Yu et al. 2017).

To calculate alpha diversity, the OTU tables for each experiment were rarefied 100 times to even depth (multiple_rarefactions_even_depth), alpha diversity was estimated and collated (scripts alpha_diversity and collate_alpha), and the mean for each sample-metric combination was calculated (plotted in supplementary figs. S5 and S11, Supplementary Material online). To test whether there was an effect of cluster (second colonization) or galactitol concentration (galactitol supplementation experiment), we used linear mixed effects models with mouse as a random effect.

For the second colonization, UPGMA clustering identified two main clusters (fig. 6). Thus, we then used linear discriminant analysis effect size (LefSe) to identify if there were any taxa that were differentially abundant between the two clusters (Segata et al. 2011). The input data for LefSe (supplementary fig. S10, Supplementary Material online) was obtained after filtering the 97% OTUs for those that were present in at least six samples (i.e., at least three mice) and at a frequency that was above 0.5%, which corresponds to ~100 reads.

Furthermore, for the galactitol supplementation experiment, we used the R package phyloseq (McMurdie and Holmes 2013) to compute the following beta-diversity metrics: Jaccard index, Bray–Curtis, unweighted and weighted UniFrac. We then tested for an effect of galactitol concentration on each beta-diversity matrix with PERMANOVA by using the adonis function with the vegan R package, with 1,000 permutations (Anderson 2001; Oksanen et al. 2009). These procedures were applied to data from day 3, 4, and 7 postcolonization or each of the last 3 days separately (as shown in supplementary figs. S6–S9, Supplementary Material online).

Natural Fecal Isolates Collection and Phenotyping

Fecal samples were collected from nine specific pathogen free mice of different litters (strain C57BC-67) and from nine healthy humans. Samples were weighted and resuspended in PBS with 15% glycerol before storage at −80 °C. To isolate lactose fermenting Enterobacteriaceae (red colonies), appropriate dilutions of the fecal samples were plated on MacConkey plates supplemented with 0.4% lactose and incubated overnight at 37 °C. The frequency of *gat*-positive bacteria among the lactose fermenting Enterobacteriaceae was estimated by replica-plating ~96 isolated clones on M9 minimal medium supplemented with 0.4% galactitol. The M9 agar plates were incubated at 30 °C and bacterial growth was scored after 24, 48, 72, and 96 h. The ability to metabolize galactitol was tested by three independent trials.

Statistical Analysis

To analyze temporal dynamics data, we used linear mixed models, with mouse as a random effect. Where required, data were transformed to meet assumptions made by parametric statistics. All analysis were performed in R (R Core Team 2016).

Supplementary Material

Supplementary data are available at *Molecular Biology and Evolution* online.

Author Contributions

I.G. and A.S. designed the study with input from R.R. A.S., R.R., J.B., M.L., and D.G. performed the experiments. A.S., R.R., M.L., and I.G. analyzed the data and wrote the manuscript.

Acknowledgments

We thank Karina Xavier, Luis Teixeira, Ivo Chelo, Armand Leroy, Christian Schlötterer, Michael Lassig and Jan Engelstaedter for discussions throughout this work. We thank Donald Court for kindly providing strain XTL298. We thank the Gene Expression, Flow Cytometry and Bioinformatics Units of the Instituto Gulbenkian de Ciência for technical support. This research received funding from the European Research Council (ERC): ERC-StG-ECOADAPT; University of Cologne-Instituto Gulbenkian de Ciência, under SFB of DFG. The authors have no conflict of interest to report. The sequence data are available from https://www.ncbi.nlm.nih.gov/bioproject/PRJNA295680 (last accessed August 18, 2017).

References

Anderson MJ. 2001. A new method for non-parametric multivariate analysis of variance: non-parametric manova for ecology. *Austral Ecol*. 26(1):32–46.

Andersson DI, Hughes D. 2010. Antibiotic resistance and its cost: is it possible to reverse resistance?. *Nat Rev Microbiol*. [Internet] Available from: http://www.nature.com/doifinder/10.1038/nrmicro2319

Barrick JE, Kauth MR, Strelioff CC, Lenski RE. 2010. *Escherichia coli* rpoB mutants have increased evolvability in proportion to their fitness defects. *Mol Biol Evol*. 27(6):1338–1347.

Barroso-Batista J, Demengeot J, Gordo I. 2015. Adaptive immunity increases the pace and predictability of evolutionary change in commensal gut bacteria. *Nat Commun*. 6:8945.

Barroso-Batista J, Sousa A, Lourenço M, Bergman M-L, Sobral D, Demengeot J, Xavier KB, Gordo I. 2014. The first steps of adaptation of *Escherichia coli* to the gut are dominated by soft sweeps. *PLoS Genet*. 10(3):e1004182.

Björkman J, Nagaev I, Berg OG, Hughes D, Andersson DI. 2000. Effects of environment on compensatory mutations to ameliorate costs of antibiotic resistance. *Science* 287(5457):1479–1482.

Blattner FR, Plunkett G, Bloch CA, Perna NT, Burland V, Riley M, Collado-Vides J, Glasner JD, Rode CK, Mayhew GF, et al. 1997. The complete genome sequence of *Escherichia coli* K-12. *Science* 277(5331):1453–1462.

Caporaso JG, Kuczynski J, Stombaugh J, Bittinger K, Bushman FD, Costello EK, Fierer N, Peña AG, Goodrich JK, Gordon JI, et al. 2010. QIIME allows analysis of high-throughput community sequencing data. *Nat Methods* 7(5):335–336.

Caporaso JG, Lauber CL, Walters WA, Berg-Lyons D, Huntley J, Fierer N, Owens SM, Betley J, Fraser L, Bauer M, et al. 2012. Ultra-high-throughput microbial community analysis on the Illumina HiSeq and MiSeq platforms. *ISME J*. 6(8):1621–1624.

Caporaso JG, Lauber CL, Walters WA, Berg-Lyons D, Lozupone CA, Turnbaugh PJ, Fierer N, Knight R. 2011. Global patterns of 16S rRNA diversity at a depth of millions of sequences per sample. *Proc Natl Acad Sci U S A*. 108(Suppl 1):4516–4522.

Caugant DA, Levin BR, Selander RK. 1981. Genetic diversity and temporal variation in the *E. coli* population of a human host. *Genetics* 98(3):467–490.

Chattopadhyay S, Weissman SJ, Minin VN, Russo TA, Dykhuizen DE, Sokurenko EV. 2009. High frequency of hotspot mutations in core genes of *Escherichia coli* due to short-term positive selection. *Proc Natl Acad Sci U S A*. 106(30):12412–12417.

Chesson P. 2000. Mechanisms of maintenance of species diversity. *Annu Rev Ecol Syst* 31(1):343–366.

Chou H-H, Chiu H-C, Delaney NF, Segrè D, Marx CJ. 2011. Diminishing returns epistasis among beneficial mutations decelerates adaptation. *Science* 332(6034):1190–1192.

Clemente JC, Ursell LK, Parfrey LW, Knight R. 2012. The impact of the gut microbiota on human health: an integrative view. *Cell* 148(6):1258–1270.

Comeau AM, Douglas GM, Langille MGI. 2017. Microbiome helper: a custom and streamlined workflow for microbiome research. *mSystems* 2:e00127-16.

Conway T, Cohen PS. 2015. Commensal and pathogenic Escherichia coli metabolism in the gut. In: Conway T, Cohen PS, editors. Metabolism and bacterial pathogenesis. American Society of Microbiology. p. 343–362. Available from: http://www.asmscience.org/content/book/10.1128/9781555818883.chap16

Couce A, Tenaillon OA. 2015. The rule of declining adaptability in microbial evolution experiments. *Front Genet*. 6:99.

Coyte KZ, Schluter J, Foster KR. 2015. The ecology of the microbiome: networks, competition, and stability. *Science* 350(6261):663–666.

Datsenko KA, Wanner BL. 2000. One-step inactivation of chromosomal genes in *Escherichia coli* K-12 using PCR products. *Proc Natl Acad Sci U S A*. 97(12):6640–6645.

David LA, Maurice CF, Carmody RN, Gootenberg DB, Button JE, Wolfe BE, Ling AV, Devlin AS, Varma Y, Fischbach MA, et al. 2014. Diet rapidly and reproducibly alters the human gut microbiome. *Nature* 505(7484):559–563.

De Paepe M, Gaboriau-Routhiau V, Rainteau D, Rakotobe S, Taddei F, Cerf-Bensussan N. 2011. Trade-off between bile resistance and nutritional competence drives *Escherichia coli* diversification in the mouse gut. *PLoS Genet*. 7:e1002107.

Deatherage DE, Barrick JE. 2014. Identification of mutations in laboratory-evolved microbes from next-generation sequencing data using breseq. In: Sun L, Shou W, editors. Engineering and analyzing multicellular systems. Vol. 1151. New York, NY: Springer. p. 165–188. Available from: http://link.springer.com/10.1007/978-1-4939-0554-6_12

DeSantis TZ, Hugenholtz P, Larsen N, Rojas M, Brodie EL, Keller K, Huber T, Dalevi D, Hu P, Andersen GL. 2006. Greengenes, a chimera-checked 16S rRNA gene database and workbench compatible with ARB. *Appl Environ Microbiol*. 72(7):5069–5072.

Dinan TG, Cryan JF. 2017. Gut–brain axis in 2016: Brain–gut–microbiota axis: mood, metabolism and behaviour. *Nat Rev Gastroenterol Hepatol*. 14(2):69–70.

Faith JJ, Ahern PP, Ridaura VK, Cheng J, Gordon JI. 2014. Identifying gut microbe-host phenotype relationships using combinatorial communities in gnotobiotic mice. *Sci Transl Med*. 6(220):220ra11.

Friedrich TC, Dodds EJ, Yant LJ, Vojnov L, Rudersdorf R, Cullen C, Evans DT, Desrosiers RC, Mothé BR, Sidney J, et al. 2004. Reversion of CTL escape: variant immunodeficiency viruses in vivo. *Nat Med*. 10(3):275–281.

Gerrish PJ, Lenski RE. 1998. The fate of competing beneficial mutations in an asexual population. *Genetica* 102–103:127–144.

Gould SJ. 1970. Dollo on Dollo's law: irreversibility and the status of evolutionary laws. *J Hist Biol*. 3:189–212.

Greenblum S, Carr R, Borenstein E. 2015. Extensive strain-level copy-number variation across human gut microbiome species. *Cell* 160(4):583–594.

Hall BM, Ma C-X, Liang P, Singh KK. 2009. Fluctuation AnaLysis CalculatOR: a web tool for the determination of mutation rate using Luria-Delbruck fluctuation analysis. *Bioinformatics* 25(12):1564–1565.

Hansen SR, Hubbell SP. 1980. Single-nutrient microbial competition: qualitative agreement between experimental and theoretically forecast outcomes. *Science* 207(4438):1491–1493.

Hegreness M, Shoresh N, Hartl D, Kishony R. 2006. An equivalence principle for the incorporation of favorable mutations in asexual populations. *Science* 311(5767):1615–1617.

Horiuchi T, Tomizawa JI, Novick A. 1962. Isolation and properties of bacteria capable of high rates of beta-galactosidase synthesis. *Biochim Biophys Acta* 55:152–163.

Khan AI, Dinh DM, Schneider D, Lenski RE, Cooper TF. 2011. Negative epistasis between beneficial mutations in an evolving bacterial population. *Science* 332(6034):1193–1196.

Krogfelt KA, Cohen PS, Conway T. 2004. The life of commensal *Escherichia coli* in the mammalian intestine. *EcoSal plus [Internet]*

1: Available from: http://www.asmscience.org/content/journal/ecosalplus/10.1128/ecosalplus.8.3.1.2
Krogfelt KA, Cohen PS, Conway T. 2013. The life of commensal *Escherichia coli* in the mammalian intestine. *EcoSal plus [Internet]* 1: Available from: http://www.asmscience.org/content/journal/ecosalplus/10.1128/ecosalplus.8.3.1.2
Kryazhimskiy S, Rice DP, Jerison ER, Desai MM. 2014. Microbial evolution. Global epistasis makes adaptation predictable despite sequence-level stochasticity. *Science* 344(6191): 1519–1522.
Lee H, Popodi E, Tang H, Foster PL. 2012. Rate and molecular spectrum of spontaneous mutations in the bacterium *Escherichia coli* as determined by whole-genome sequencing. *Proc Natl Acad Sci U S A*. 109(41):E2774–E2783.
Li X.-t, Thomason LC, Sawitzke JA, Costantino N, Court DL. 2013. Positive and negative selection using the tetA-sacB cassette: recombineering and P1 transduction in *Escherichia coli*. *Nucleic Acids Res*. 41(22):e204–e204.
Lourenço M, Ramiro RS, Güleresi D, Barroso-Batista J, Xavier KB, Gordo I, Sousa A. 2016. A mutational hotspot and strong selection contribute to the order of mutations selected for during *Escherichia coli* adaptation to the gut. *PLoS Genet*. 12:e1006420.
Lozupone C, Knight R. 2005. UniFrac: a new phylogenetic method for comparing microbial communities. *Appl Environ Microbiol*. 71(12):8228–8235.
Marshall CR, Raff EC, Raff RA. 1994. Dollo's law and the death and resurrection of genes. *Proc Natl Acad Sci U S A*. 91(25):12283–12287.
McMurdie PJ, Holmes S. 2013. phyloseq: An R package for reproducible interactive analysis and graphics of microbiome census data. *PLoS One* 8:e61217.
Nayfach S, Rodriguez-Mueller B, Garud N, Pollard KS. 2016. An integrated metagenomics pipeline for strain profiling reveals novel patterns of bacterial transmission and biogeography. *Genome Res*. 26(11):1612–1625.
Ning Z, Cox AJ, Mullikin JC. 2001. SSAHA: a fast search method for large DNA databases. *Genome Res*. 11(10):1725–1729.
van Nood E, Vrieze A, Nieuwdorp M, Fuentes S, Zoetendal EG, de Vos WM, Visser CE, Kuijper EJ, Bartelsman JFWM, Tijssen JGP, et al. 2013. Duodenal infusion of donor feces for recurrent *Clostridium difficile*. *N Engl J Med*. 368(5):407–415.
Oksanen J, Kindt R, Legendre P, O'Hara B, Simpson GL, Stevens MHH, Wagner H. 2009. Vegan: community ecology package. R package version 2.9. 2.
van Opheusden JHJ, Hemerik L, van Opheusden M, van der Werf W. 2015. Competition for resources: complicated dynamics in the simple Tilman model. *SpringerPlus [Internet]* 4(1). Available from: http://www.springerplus.com/content/4/1/474
Porter ML, Crandall KA. 2003. Lost along the way: the significance of evolution in reverse. *Trends Ecol Evol*. 18(10):541–547.
Poulsen LK, Licht TR, Rang C, Krogfelt KA, Molin S. 1995. Physiological state of *Escherichia coli* BJ4 growing in the large intestines of streptomycin-treated mice. *J Bacteriol*. 177(20):5840–5845.
R Core Team. 2016. R: A language and environment for statistical computing. Vienna, Austria: R Foundation for Statistical Computing. Available from: https://www.R-project.org/
Rang CU, Licht TR, Midtvedt T, Conway PL, Chao L, Krogfelt KA, Cohen PS, Molin S. 1999. Estimation of growth rates of *Escherichia coli* BJ4 in streptomycin-treated and previously germfree mice by in situ rRNA hybridization. *Clin Diagn Lab Immunol*. 6(3):434–436.
Robinson JT, Thorvaldsdóttir H, Winckler W, Guttman M, Lander ES, Getz G, Mesirov JP. 2011. Integrative genomics viewer. *Nat Biotechnol*. 29(1):24–26.
Salter SJ, Cox MJ, Turek EM, Calus ST, Cookson WO, Moffatt MF, Turner P, Parkhill J, Loman NJ, Walker AW. 2014. Reagent and laboratory contamination can critically impact sequence-based microbiome analyses. *BMC Biol [Internet]* 12(1).Available from: http://bmcbiol.biomedcentral.com/articles/10.1186/s12915-014-0087-z
Schloissnig S, Arumugam M, Sunagawa S, Mitreva M, Tap J, Zhu A, Waller A, Mende DR, Kultima JR, Martin J, et al. 2013. Genomic variation landscape of the human gut microbiome. *Nature* 493(7430):45–50.
Segata N, Izard J, Waldron L, Gevers D, Miropolsky L, Garrett WS, Huttenhower C. 2011. Metagenomic biomarker discovery and explanation. *Genome Biol*. 12(6):R60.
Thompson JA, Oliveira RA, Djukovic A, Ubeda C, Xavier KB. 2015. Manipulation of the quorum sensing signal AI-2 affects the antibiotic-treated gut microbiota. *Cell Rep*. 10(11):1861–1871.
de Visser JAGM, Krug J. 2014. Empirical fitness landscapes and the predictability of evolution. *Nat Rev Genet*. 15(7):480–490.
Waldor MK, Tyson G, Borenstein E, Ochman H, Moeller A, Finlay BB, Kong HH, Gordon JI, Nelson KE, Dabbagh K, et al. 2015. Where next for microbiome research?. *PLoS Biol*. 13(1):e1002050.
Wilson K. 2001. Preparation of genomic DNA from bacteria. In: Ausubel FM, Brent R, Kingston RE, Moore DD, Seidman JG, Smith JA, Struhl K, editors. Current protocols in molecular biology. Hoboken, NJ, USA: John Wiley & Sons, Inc. p. 2.4.1–2.4.5. Available from: http://doi.wiley.com/10.1002/0471142727.mb0204s56
Yu G, Smith DK, Zhu H, Guan Y, Lam TT-Y. 2017. Package for visualization and annotation of phylogenetic trees with their covariates and other associated data. *Methods Ecol Evol*. 8:28–36.
Zhong S, Khodursky A, Dykhuizen DE, Dean AM. 2004. Evolutionary genomics of ecological specialization. *Proc Natl Acad Sci U S A*. 101(32):11719–11724.
Zhong S, Miller SP, Dykhuizen DE, Dean AM. 2009. Transcription, translation, and the evolution of specialists and generalists. *Mol Biol Evol*. 26(12):2661–2678.